PERGAMON

Journal of Structural Geology 25 (2003) 1569–1574

JOURNAL OF STRUCTURAL GEOLOGY

www.elsevier.com/locate/jsg

Fractal dimension of molten surfaces as a possible parameter to infer the slip-weakening distance of faults from natural pseudotachylytes

Takehiro Hirose*, Toshihiko Shimamoto

Department of Geology and Mineralogy, Division of Earth and Planetary Sciences, Graduate School of Science, Kyoto University, Kyoto 606-8502, Japan

Received 9 June 2002; received in revised form 23 December 2002; accepted 13 January 2003

Abstract

High-velocity friction experiments on gabbro and monzodiorite, using a rotary-shear high-velocity friction apparatus, have revealed that frictional melting and progressive growth of a molten layer along a fault cause slip weakening, eventually reaching a nearly steady-state. The melting surface at the host rock/molten layer interface is initially very flat, but it becomes more complex and rounded in shape towards the steady state owing to the selective melting of minerals with lower melting points and the Gibbs–Thomson effect. This change in the melting-surface topography can be quantitatively expressed by the fractal dimension D, as determined by the divider method, from about 1.0 near the peak friction to around 1.1 near the steady-state friction. The ultimate fractal dimension at steady-state friction tends to decrease with increasing heat production rate presumably due to more rapid and uniform melting. A systematic correlation of D with mechanical behavior of the fault during frictional melting may provide a way of estimating slip-weakening distance and heat production rate at steady-state friction by measuring D for natural pseudotachylytes on slip surfaces with different displacements. The weakening distance is of vital significance in relation to fault instability and the heat production rate is related to the fault strength. The experimental studies point to ways to estimate these difficult quantities for natural faults.

Keywords: Pseudotachylyte; Frictional melting; Fractal surface; Slip weakening; Fault instability; Seismic fault motion

1. Introduction

Pseudotachylytes are often cited as evidence of seismic fault motion and have been described in detail (e.g. Sibson 1975; Magloughlin and Spray, 1992; Spray 1993). Frictional melting experiments have reproduced natural pseudotachylytes successfully in regard to overall textures, chemistry, non-equilibrium nature of frictional melting, size-distribution of clasts and temperature rise during melting (Spray 1987, 1988; Shimamoto and Lin, 1994; Tsutsumi and Shimamoto 1997a; Lin and Shimamoto 1998; Tsutsumi 1999). Tsutsumi and Shimamoto (1997b) also demonstrated marked high-velocity weakening of faults during frictional melting. Despite these works, it is still difficult to infer fault properties from natural pseudotachylytes relevant to earthquake generation.

We have been trying to identify underlying physical processes that determine mechanical properties of faults during frictional melting by further laboratory experiments (Hirose et al., 2000; Hirose, 2002). Understanding the physical processes is essential for the correct application of laboratory data to natural faults since laboratory and natural conditions are not the same. Through this study, we have recognized a systematic evolution in the topography of the melting surface that can be correlated with the mechanical behavior of faults (Hirose and Shimamoto, 2001). This paper reports the change in the topography in terms of fractal dimension (Mandelbrot, 1982; Turcotte, 1997) and proposes a method to infer the slip-weakening distance, a critical parameter for fault instability (e.g. Scholz, 1990; Ohnaka, 1992), and the heat production rate from natural pseudotachylytes.

2. Experimental procedures

All experiments were conducted under dry conditions, at room temperature, slip rates of 0.85–1.6 m/s and normal

* Corresponding author. Now at: Geologisches Institut, ETH-Zentrum, CH-8092, Zurich, Switzerland. Fax: +41-1-632-3709.
E-mail address: hirose@erdw.ethz.ch (T. Hirose).

0191-8141/03/$ - see front matter © 2003 Elsevier Science Ltd. All rights reserved.
doi:10.1016/S0191-8141(03)00009-9

stresses of 1.25–2.19 MPa, using a rotary-shear, high-speed frictional testing apparatus described by Shimamoto and Tsutsumi (1994). A pair of 25-mm-long hollow-cylindrical specimens with outer and inner diameters of 25 and 15 mm, respectively, are pressed together with an air-pressure driven actuator, and the specimen on one side is rotated at revolution rates up to 1500 rpm with a 7.5 kW motor while the other side is kept stationary. Hollow cylindrical specimens are used to minimize the gradient in slip rate; 1.96 m/s at the outer wall and 1.18 m/s at the inner wall for our specimens. In this paper we use 'equivalent velocity', v_{eq}, defined such that $\tau v_{eq} S$ gives the rate of total frictional work on a fault with area S under the assumption of no velocity dependence of the shear stress τ (Shimamoto and Tsutsumi, 1994). The equivalent velocity (simply called velocity or slip rate hereafter) is 1.60 m/s at 1500 rpm revolution rate, and this is the maximum slip rate in our experiments.

We used gabbro from India and monzodiorite from Zimbabwe with average grain sizes of 0.51 and 0.26 mm, respectively, in our experiments. Major constituent minerals of the gabbro are plagioclase, clinopyroxene, hornblende, biotite, ilmenite and hematite, whereas those of the monzodiorite are plagioclase, hornblende, biotite, muscovite, quartz and opaque minerals affected by alteration. The outside surfaces and ends of hollow-cylindrical specimens were ground with a 400#-grit diamond grinding machine using a cylindrical grinder. A difficulty in high-velocity friction experiments is severe thermal fracturing, which can lower the uniaxial strength of rocks by more than two orders of magnitude (Ohtomo and Shimamoto, 1994). These rocks were selected since they are less affected by thermal fracturing than rocks containing significant amounts of quartz that undergo the α–β transformation. Even for gabbroic rocks we could only apply normal stresses up to about 2.0 MPa. Thus the heat production rate in our experiments is much smaller than expected for deeper faults, so that displacements on the order of 100 m are required to see the entire spectrum of behavior associated with frictional melting. Hence our experiments use displacements up to 117 m to produce the same order of total frictional heat as expected at greater depths, as a trade-off for the effects of deeper, higher normal-stress faulting.

Experimentally generated pseudotachylytes along simulated faults were thin sectioned parallel to the slip direction as closely as possible in order to observe the microstructures under an optical microscope and an analytical SEM.

3. Experimental results

Fig. 1 shows a typical, high-velocity behavior of gabbro, as expressed by a frictional coefficient vs. displacement curve. There are two stages of slip weakening (potential sites for unstable fault motion; e.g. Scholz, 1990); one after the frictional peaks (A to B) and the other following the

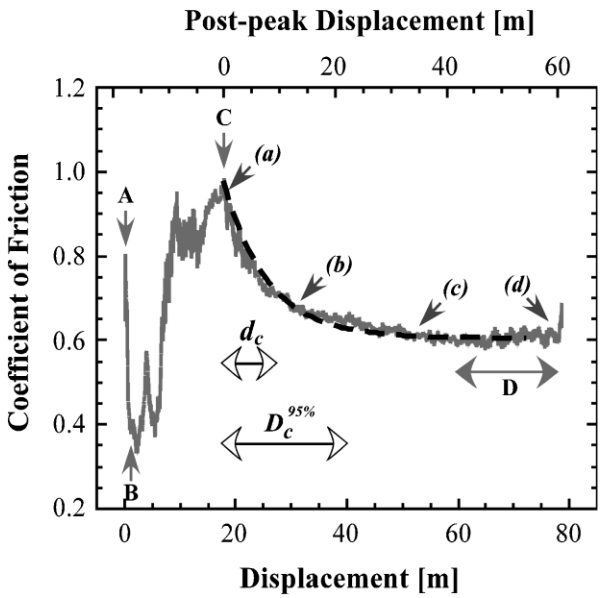

Fig. 1. A representative frictional behavior of gabbro at a slip rate of 0.85 m/s and a normal stress of 1.25 MPa, shown as a frictional coefficient vs. displacement curve. Two stages of slip weakening are recognized (A to B and C to D). Dashed line is a least-squares fit to the second slip-weakening using Kaleida Graph software with parameters and standard errors: frictional coefficient at the second peak friction, $\mu_{max} = 0.86 \pm 0.001$, frictional coefficient at the steady-state or residual friction, $\mu_{ss} = 0.6 \pm 0.0005$, and the slip-weakening parameter, $d_c = 9.4 \pm 0.08$ m. Arrow points, (a) to (d), indicated post-peak displacements corresponding to the four experiments shown in Figs. 2 and 3.

second peak friction (C to D). Friction decreases exponentially during the second slip weakening (Fig. 1), and the weakening behavior can be fit by an empirical equation:

$$\mu = \mu_{ss} + (\mu_{max} - \mu_{ss})\exp(-d/d_c) \quad (1)$$

where the μ_{max} and μ_{ss} are frictional coefficients at the second peak friction and at the residual or steady-state friction, respectively, d is displacement after the second peak friction and d_c is a constant. The slip-weakening parameter, d_c, is defined as the post-peak displacement at which $(\mu - \mu_{ss})$ reduces to $\exp(-1) \sim 0.368$ of $(\mu_{max} - \mu_{ss})$. The slip-weakening parameter for data in Fig. 1 is 9.4 ± 0.08 m.

Melt patches begin to form soon after B in Fig. 1 and the accumulation of melt patches induces marked strengthening of the fault from B to C, presumably because very thin, viscous melt patches impose high viscous drag owing to large shear strain rate of the melt patches (Hirose, 2002). A thin, but continuous molten layer forms along the fault at around the second peak friction (C), and this is followed by slip weakening associated with frictional melting towards the steady-state or residual friction (D). A continuous molten layer forms after the second peak friction so that post-second-peak behavior is relevant to the pseudotachylyte formation. This paper is thus concerned with the evolution of this continuous molten layer (from C to D in Fig. 1). We firstly present data from eight experiments on

gabbro under the same conditions as those for the run shown in Fig. 1 (slip rate = 0.85 m/s, normal stress = 1.25 MPa), but each run was stopped at a different displacement to see how the development of the molten layer is correlated with the mechanical behavior of the fault. Fig. 2 shows representative sketches and corresponding photomicrographs of simulated faults for (a) just after the second peak friction, (b) post-peak regime, (c) pre-residual regime and (d) steady-state or residual regime. The overall behavior is reproduced reasonably well in these runs although the displacement at the second peak friction varies from 17 to 23 m (Hirose, 2002). Thus the displacement after this peak (post-peak displacement) is used as a reference displacement for the runs as shown by (a) to (d) in Fig. 1, corresponding to the sketches and photomicrographs in Fig. 2. Experimentally generated pseudotachylytes consist of melt, bubbles coming from hydrous minerals and clasts or rock fragments (see Fig. 2).

The molten layer is very thin, locally on the order of microns near the second peak friction, but it is continuous along the fault and no direct host-rock contacts across the fault were recognized under an optical microscope. Hence from this stage onwards, the source of frictional heating is primarily the viscous shear heating of the molten zone containing bubbles and clasts. Melting then occurs from surfaces of host rock and from the surface of clasts to produce a more irregular and curvaceous surface of host rock and clasts, often with embayments, towards the steady-

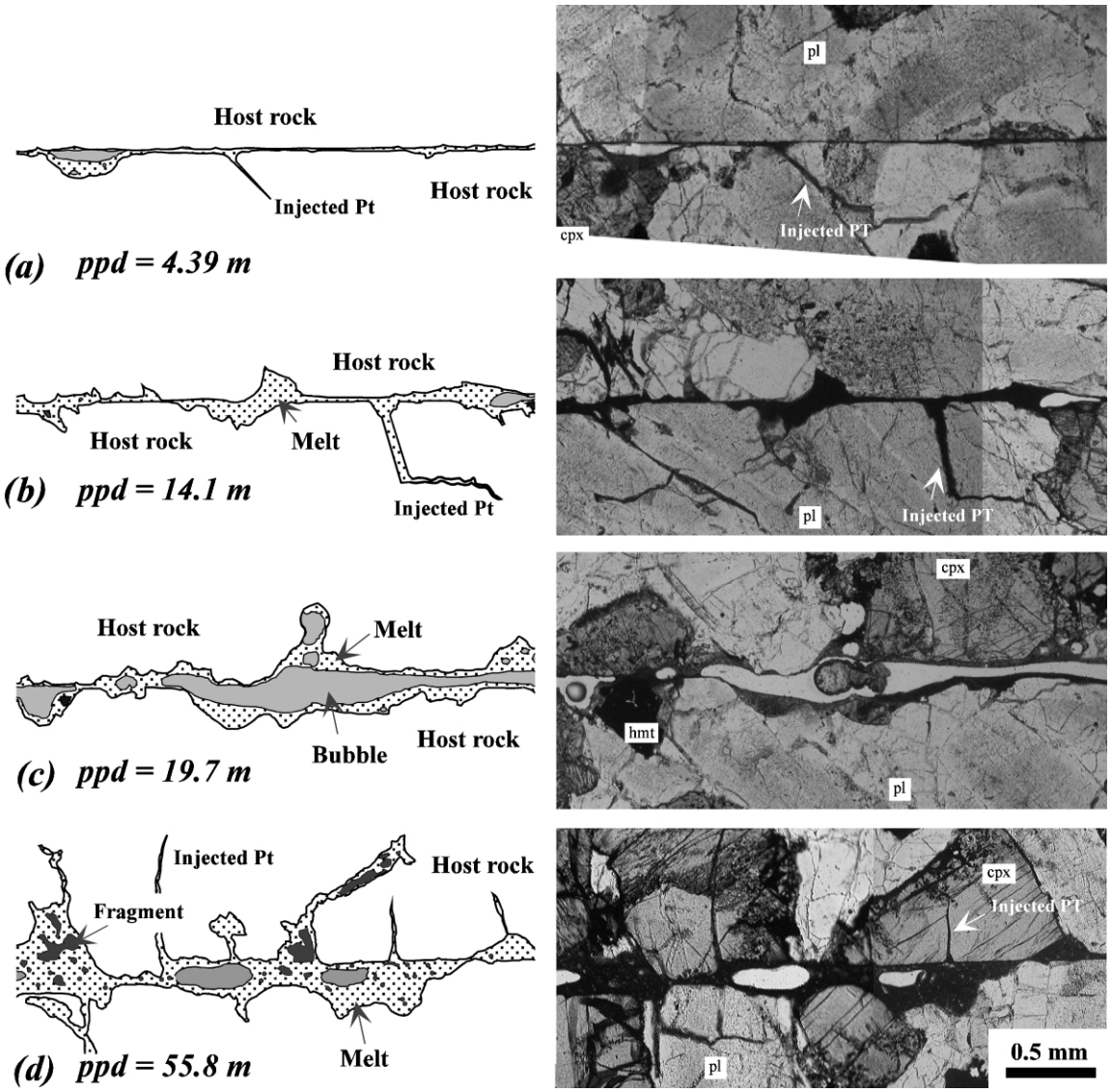

Fig. 2. Representative sketches (left) and corresponding photomicrographs under plane-polarized light (right) showing experimentally generated pseudotachylyte in gabbro, just after the second peak friction (a) towards the steady-state or residual friction (d). Molten layers (stippled portions) contain bubbles (fine stippled portions) and fragments (filled portions). Host-rock/molten-layer interfaces are shown as solid lines. All experiments were done under the same conditions as for the run in Fig. 1, but with different displacements. The post-peak displacements (ppd) at the end of each experiment for specimens (a)–(d) are shown in Fig. 1 by corresponding symbols. Melt is locally injected into host rock as denoted by 'injected PT'. (cpx: clinopyroxene, pl: plagioclase, hmt: hematite).

state friction regime as seen from (a) to (d) in Fig. 2. Clast content in the molten zone continues to increase as the fault reaches a mechanical steady state so that spalling off of the host rock must be taking place from irregular and embayed surfaces to form clasts.

To quantify the change in topography of melting surface, fractal analyses have been conducted on the melting surface in the eight specimens, using a standard divider method, in a manner similar to that used to analyze coastlines (Mandelbrot, 1982; Turcotte, 1997). A linear relationship holds between the logarithm of the divider length and the logarithm of the total length of the melting surfaces, as shown for four representative samples in Fig. 3. The surface topography can then be expressed by the fractal dimension D, given by $1 - M$, where M is the slope of these lines. D is shown in Fig. 4a as a function of the post-peak displacement on the lower horizontal axis. The fault surface is very straight and flat ($D = 1.0$) near the second peak friction, more or less the same as the ground initial surface. The fractal dimension increases first rapidly and then changes gradually towards a constant value of around 1.1 in the nearly steady-state friction stage (called 'steady-state fractal dimension', D_{ss}; Fig. 4a). The change in the fractal dimension can be expressed well with an equation:

$$D = D_{ss} + (D_0 - D_{ss})\exp\left(-d/d_c^{fractal}\right) \quad (2)$$

where d is the post-peak displacement and $d_c^{fractal}$ is a constant that specifies how rapidly D approaches D_{ss}. The fractal change parameter, $d_c^{fractal}$, is 7.5 ± 2.3 m for data in Fig. 4a (dashed line in the figure).

We secondly present data from six experiments for gabbro and monzodiorite specimens allowed to continue slipping until steady-state friction was reached. The steady-state shear stress data were used to calculate heat production rate per unit fault area (shear stress multiplied by the equivalent velocity), assuming that all frictional work changes into heat. Fig. 4b shows that the steady-state fractal dimension of melting surface decreases with increasing steady-state heat production rate and that there is a strong influence of lithology in this relationship.

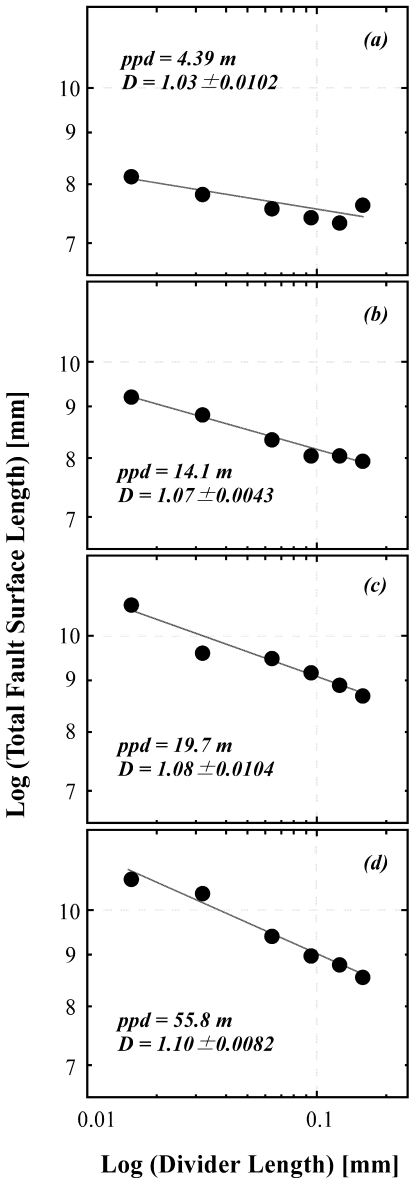

Fig. 3. Fractal analyses of the melting surfaces at host-rock/molten-layer interfaces for four gabbro specimens in Fig. 2 (ppd: post-peak displacement), using a divider method (Mandelbrot, 1982). The vertical axis gives the total length of melting surface as measured by a divider whose length is shown on the horizontal axis, and the fractal dimension, D, is the slope of their linear relationship. The values of D and its standard errors were calculated by the least-squares method using Kaleida Graph software. The analyses were done for the entire melting surfaces in thin sections, much longer than the melting surfaces shown in Fig. 2.

4. Discussion

The slip weakening following the second peak friction is accompanied by the development of a more irregular, round-shaped and embayed melting surface towards the steady-state or residual friction, corresponding to a change in fractal dimension from 1.0 to about 1.1 (Fig. 4a). The progressive development of irregular surfaces is most likely due to heterogeneous and/or selective melting on the surface; mafic minerals tend to melt faster than plagioclase. The Gibbs–Thomson effect can be another cause for making melting surface round shaped; i.e. the local melting temperature at a curved mineral surface sticking out into the melt is lowered by an amount proportional to the ratio of surface tension to the latent heat and also proportional to the mean curvature (Alexiades and Solomon, 1993, p. 80). The drop in melting temperature cannot be estimated because surface tension is not known. But the temperature drop is large for sharp sticking-out corners because of its large curvature, so that sharp corners preferentially melt to produce round-shaped melting surfaces. Likewise, if a grain contains a crack, sharp corners created by the crack will preferentially melt and melting will proceed into the crack

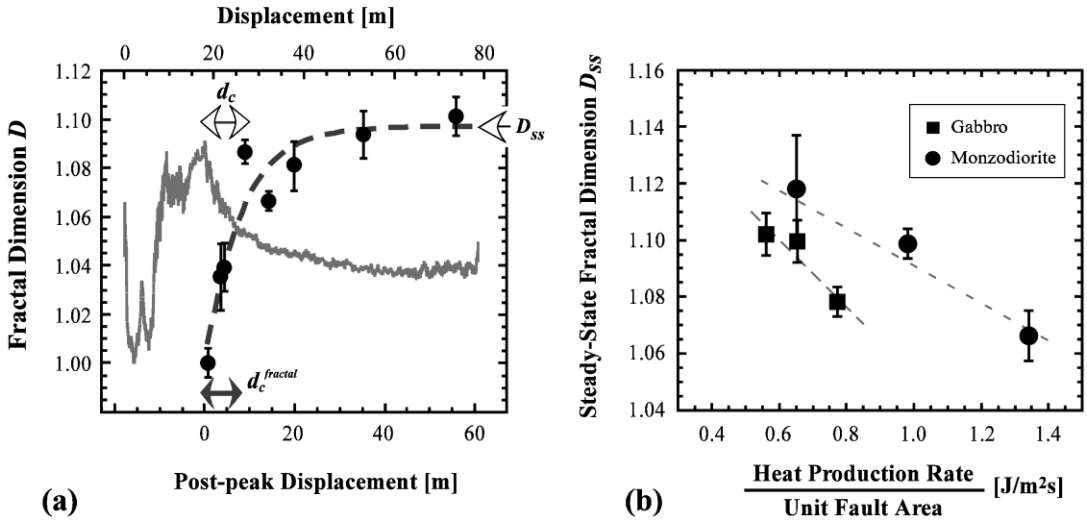

Fig. 4. (a) Fractal dimension D of melting surface for eight gabbro specimens, plotted against the post-peak displacement and (b) steady-state fractal dimension D_{ss} for gabbro and monzodiorite specimens, plotted against the heat-production rate per unit fault area at the steady-state or residual friction. Experiments for (a) were done under the same conditions as that shown in Fig. 1, but those for (b) were done with different slip rates and normal stresses to change the heat production rate. A thin curve in (a) is the frictional coefficient vs. displacement curve in Fig. 1 for comparison of D with a typical mechanical behavior. Dashed line in (a) is a least-squares fit to the fractal data with Eq. (2) using Kaleida Graph software with parameters and standard errors: initial fractal dimension, $D_0 = 1.0$, steady-state fractal dimension, $D_{ss} = 1.09 \pm 0.01$, and fractal change parameter, $d_c^{fractal} = 7.5 \pm 2.3$ m. The least-squares fit of the form Eq. (2) gives $D_0 = 0.97 \pm 0.02$, unreasonable for the fractal dimension. Thus we fixed $D_0 = 1.0$ based on the fractal analysis as in Fig. 3 for the initial point, which yields a fractal dimension of 0.996 ± 0.006 and determined other parameters in Eq. (2) by the least-squares method.

leaving round-shaped corners behind (see cpx grain on the upper right side of Fig. 2d).

The steady-state fractal dimension tends to decrease with increasing heat production rate (Fig. 4b). The reason for this trend is not understood well, but we suggest that a higher rate of heat production enhances the rate of frictional melting, which suppresses the selective and heterogeneous melting, thereby creating a smoother surface. We assumed that all frictional work goes into heat in Fig. 4b. This probably is not a bad assumption because Lockner and Okubo (1983) showed experimentally that $94 \pm 2\%$ of frictional work goes into heat.

Slip-weakening distance, D_c, is a very important parameter for fault instability (e.g. Scholz, 1990; Ohnaka, 1992). This distance is normally defined as 'slip distance from peak friction to the steady-state friction'. We have used a slip weakening parameter, d_c, in Eq. (1), because it is a very useful parameter to specify exponential curves. The displacement at which steady state is attained cannot be determined precisely for an exponential-type decay of μ (or mathematically it has to be infinite). Thus we define a conventional slip-weakening distance as a post-peak displacement at which $(\mu - \mu_{ss})$ reduces to 0.05 of $(\mu_{max} - \mu_{ss})$. Eq. (1) yields $D_c^{95\%} \sim 3d_c$ (Fig. 1). This quantity will be closer to the slip-weakening distance in its ordinary definition. Hirose (2002) has shown that slip weakening is primarily caused by growth of a molten layer that lowers the shear strain rate for a given slip rate. Melt moves more easily along a fault as the molten layer grows and the steady state is attained when rate of melt production is balanced with the rate of melt loss. These processes will be discussed in more detail elsewhere.

A striking feature of the present results is that both the fractal dimension of the melting surfaces, D, and the frictional coefficient, μ, change exponentially in very similar manners towards the steady state (cf. Eqs. (1) and (2) and Figs. 1 and 4a). The slip-weakening parameter, d_c, is 9.4 ± 0.08 m (Fig. 1) and the fractal change parameter, $d_c^{fractal}$, is 7.5 ± 2.3 m (Fig. 4a). This correlation will provide a way of estimating the slip-weakening distance for natural faults, a very difficult quantity that has not been determined as yet. A straightforward application of our results to natural pseudotachylytes is (1) to determine fractal dimension D of the melting surface of the pseudotachylyte generation zones with different fault displacements d and (3) to plot D against d. If a result similar to that in Fig. 4a is obtained, one should be able to estimate an ultimate fractal dimension at steady-state friction for natural faults and the slip-weakening parameter, d_c, by determining $d_c^{fractal}$. One should be also able to infer from the diagram what stage of mechanical behavior each pseudotachylyte experienced.

If the relationship between the steady-state fractal dimension D_{ss} and the heat production rate, such as that in Fig. 4b, is established for the host rock, the level of friction at the steady state may be estimated from the heat production rate assuming possible ranges for a seismic slip rate. However, this relationship between D_{ss} and the heat production rate must be determined by experiments for each case, because the relationship varies with rock types. A pseudotachylyte sample from the Outer Hebrides, Scotland, exhibits a fractal melting surface, very similar to that shown

herein (Hirose and Shimamoto, 2001), and systematic analysis of melting surfaces is desirable for natural pseudotachylytes.

A big controversy over the last decade is that the seismically determined slip-weakening distance is on the order of 0.5–1 m, greater than laboratory-determined values in conventional tests by several orders of magnitude (e.g. Ide and Takeo, 1997). Thus estimation of the weakening distance from natural faults will be of interest with respect to this controversy. More involved constitutive parameters, such as those of Dieterich (1981), cannot be determined with our present data on high velocity friction. Note that a parameter such as d_c in Eq. (1) changes markedly with heat production rate and there are no fixed properties to faults at high velocities (see data in Hirose 2002). Hence high velocity friction is a highly nonlinear phenomenon for which displacement and slip history themselves determine the fault properties. Close correlations between natural and experimental pseudotachylytes will be a guide for challenging this complex phenomenon.

Acknowledgements

We thank A. Tsutsumi, K. Mizoguchi and C.A.J. Wibberley for their useful discussions and S.F. Cox, L. Kennedy and C.A.J. Wibberley for their careful reviews of the manuscript.

References

Alexiades, V., Solomon, A.D., 1993. Mathematical Modeling of Melting and Freezing Processes, Hemisphere Publishing Corporation, Washington, DC.

Dieterich, J.H., 1981. Constitutive properties of faults with simulated gouge. American Geophysical Union Geophysical Monograph 24, 103–120.

Hirose, T., 2002. Experimental and field studies of frictional melting along faults and implications for earthquake generation processes. Ph.D. thesis, Kyoto University.

Hirose, T., Shimamoto, T., 2001. Fractal dimension of melting surface as a possible link between high-velocity frictional behavior of faults and natural pseudotachylytes. Global Meeting on Earth System Processes. The Geological Society of America and the Geological Society of London, Edinburgh, Scotland, Abstract, 49 pp.

Hirose, T., Tsutsumi, A., Shimamoto, T., 2000. High-velocity slip weakening on gabbro during frictional melting. Eos Transactions of the American Geophysical Union 81, Fall Meeting, San Francisco, Abstracts, 1200 pp.

Ide, S., Takeo, M., 1997. Determination of the constitutive relation of fault slip based on wave analysis. Journal of Geophysical Research 102, 27379–27392.

Lin, A., Shimamoto, T., 1998. Selective melting processes as inferred from experimentally generated pseudotachylytes. Journal of Asian Earth Science 16, 533–544.

Lockner, D.A., Okubo, P.G., 1983. Measurements of frictional heating in granite. Journal of Geophysical Research 88, 4313–4320.

Magloughlin, J.F., Spray, J.G., 1992. Frictional melting process and products in geological materials: introduction and discussion. Tectonophysics 204, 197–206.

Mandelbrot, B.B., 1982. The Fractal Geometry of Nature, W.H. Freeman and Company, New York.

Ohnaka, M., 1992. Earthquake source nucleation: a physical model for short-term precursors. Tectonophysics 211, 149–178.

Ohtomo, Y., Shimamoto, T., 1994. Significance of thermal fracturing in the generation of fault gouge during rapid fault motion: an experimental verification. Structural Geology, Journal of Tectonic Research Group of Japan 39, 135–144. (in Japanese with English abstract).

Scholz, C.H., 1990. The Mechanics of Earthquake Faulting, Cambridge University Press, Cambridge, UK.

Shimamoto, T., Lin, A., 1994. Is frictional melting equilibrium melting or non-equilibrium melting? Structural Geology, Journal of Tectonic Research Group of Japan 39, 79–84. (in Japanese with English abstract).

Shimamoto, T., Tsutsumi, A., 1994. A new rotary-shear high-speed frictional testing machine: its basic design and scope of research. Structural Geology, Journal of Tectonic Research Group of Japan 39, 65–78. (in Japanese with English abstract).

Sibson, R.H., 1975. Generation of pseudotachylyte by ancient seismic faulting. Geophysical Journal of the Royal Astronomical Society 43, 775–794.

Spray, J.G., 1987. Artificial generation of pseudotachylyte using frictional welding apparatus: simulation of melting on a fault plane. Journal of Structural Geology 9, 49–60.

Spray, J.G., 1988. Generation and crystallization of an amphibolite shear melt: an investigation using radial friction welding apparatus. Contributions to Mineralogy and Petrology 99, 464–475.

Spray, J.G., 1993. Viscosity determinations of some frictionally generated silicate melts: implications for fault zone rheology at high strain rates. Journal of Geophysical Research 98, 8053–8068.

Tsutsumi, A., 1999. Size distribution of clasts in experimentally produced pseudotachylytes. Journal of Structural Geology 21, 305–312.

Tsutsumi, A., Shimamoto, T., 1997. Temperature measurements along simulated faults during seismogenic fault motion. Proceedings of the 30th IGC, Beijing, 15, pp. 223–232.

Tsutsumi, A., Shimamoto, T., 1997b. High-velocity frictional properties of gabbro. Geophysical Research Letters 24, 699–702.

Turcotte, D.L., 1997. Fractals and Chaos in Geology and Geophysics, 2nd ed, Cambridge University Press, Cambridge, UK.